PNAS PLUS

Antiviral screening identifies adenosine analogs targeting the endogenous dsRNA *Leishmania* RNA virus 1 (LRV1) pathogenicity factor

F. Matthew Kuhlmann[a,b], John I. Robinson[a], Gregory R. Bluemling[c], Catherine Ronet[d], Nicolas Fasel[d], and Stephen M. Beverley[a,1]

[a]Department of Molecular Microbiology, Washington University School of Medicine in St. Louis, St. Louis, MO 63110; [b]Department of Medicine, Division of Infectious Diseases, Washington University School of Medicine in St. Louis, St. Louis, MO 63110; [c]Emory Institute for Drug Development, Emory University, Atlanta, GA 30329; and [d]Department of Biochemistry, University of Lausanne, 1066 Lausanne, Switzerland

Contributed by Stephen M. Beverley, December 19, 2016 (sent for review November 21, 2016; reviewed by Buddy Ullman and C. C. Wang)

The endogenous double-stranded RNA (dsRNA) virus *Leishmaniavirus* (LRV1) has been implicated as a pathogenicity factor for leishmaniasis in rodent models and human disease, and associated with drug-treatment failures in *Leishmania braziliensis* and *Leishmania guyanensis* infections. Thus, methods targeting LRV1 could have therapeutic benefit. Here we screened a panel of antivirals for parasite and LRV1 inhibition, focusing on nucleoside analogs to capitalize on the highly active salvage pathways of *Leishmania*, which are purine auxotrophs. Applying a capsid flow cytometry assay, we identified two 2′-C-methyladenosine analogs showing selective inhibition of LRV1. Treatment resulted in loss of LRV1 with first-order kinetics, as expected for random virus segregation, and elimination within six cell doublings, consistent with a measured LRV1 copy number of about 15. Viral loss was specific to antiviral nucleoside treatment and not induced by growth inhibitors, in contrast to fungal dsRNA viruses. Comparisons of drug-treated LRV1$^+$ and LRV1$^-$ lines recapitulated LRV1-dependent pathology and parasite replication in mouse infections, and cytokine secretion in macrophage infections. Agents targeting Totiviridae have not been described previously, nor are there many examples of inhibitors acting against dsRNA viruses more generally. The compounds identified here provide a key proof-of-principle in support of further studies identifying efficacious antivirals for use in in vivo studies of LRV1-mediated virulence.

trypanosomatid protozoan parasite | endobiont virus | viral segregation | chemotherapy | virulence

Protozoan parasites of the genus *Leishmania* are responsible for leishmaniasis in many regions of the world, with 12 million current cases (accompanied by at least 10-fold more bearing asymptomatic infections) and nearly 1.7 billion people at risk (1–5). The disease has three predominant clinical manifestations, ranging from the relatively mild, self-healing cutaneous form, to mucocutaneous lesions where parasites metastasize to and cause destruction of mucous membranes of the nose, mouth, and throat, or fatal visceral disease. Disease phenotypes segregate primarily with the infecting species; however, it is not fully understood which parasite factors affect severity and disease manifestations.

One recently identified parasite factor contributing to disease severity in several *Leishmania* species is the RNA virus *Leishmaniavirus* (6, 7). These endobiont viruses classified within the Totiviridae are comprised of a single-segmented double-stranded RNA (dsRNA) genome that encodes only a capsid protein and an RNA-dependent RNA polymerase (RDRP) (8, 9). *Leishmaniavirus* is most frequently found in New World parasite species in the subgenus *Viannia* [as *Leishmania* RNA virus 1 (LRV1)], such as *Leishmania braziliensis* (*Lbr*) and *Leishmania guyanensis* (*Lgy*), which cause both cutaneous and mucocutaneous disease (6), and is found sporadically in Old World subgenus *Leishmania* species [as *Leishmania* RNA virus 2 (LRV2)] (10, 11). Mice infected with LRV1-bearing strains of *L. guyanensis* exhibit greater footpad swelling and higher parasite numbers than mice infected with LRV1$^-$ *L. guyanensis* (7). Similarly, macrophages infected in vitro with LRV1$^+$ *L. guyanensis* or LRV2$^+$ *Leishmania aethiopica* release higher levels of cytokines, which are dependent on Toll-like receptor 3 (7, 10). Recently, methods for systematically eliminating LRV1 by RNA interference have been developed, enabling the generation of isogenic LRV1$^-$ lines and allowing the extension of the LRV1-dependent virulence paradigm to *L. braziliensis* (12).

A key question is the relevancy of the studies carried out in murine models to human disease. For *L. guyanensis*, patients infected with LRV1$^+$ strains show an increased severity of cutaneous disease (13). In humans, *L. braziliensis* is associated with cutaneous leishmaniasis, as well as the larger share of the more debilitating mucocutaneous leishmaniasis (MCL). Thus far there are no data available in humans permitting tests of the association of LRV1 with *L. braziliensis* parasite burden nor the severity of cutaneous leishmaniasis (CL), which can show a range of presentations (14, 15). In lieu of such information, studies have focused on the association of LRV1 with MCL vs. CL, which is thought to reflect primarily immunopathology rather than parasite numbers (2, 6, 14–16). Although in some studies LRV1 was not correlated with MCL clinical manifestations (17, 18), in others there was a strong association (6, 19, 20). The basis for these discrepancies is of considerable interest, hypotheses for which include other parasite or host factors known to play a significant role in the development of MCL (13, 21, 22), or

Significance

The endogenous double-stranded RNA virus *Leishmaniavirus* (LRV1) has been implicated as a pathogenicity factor for leishmaniasis in rodent models and human disease, and associated with drug-treatment failures. As a first step toward the identification of therapeutic LRV1 inhibitors, we identified two adenosine analogs that selectively inhibited LRV1 replication. These analogs were used as tools to confirm that viral inheritance is by random segregation, as well as to generate LRV1-cured lines of *Leishmania guyanensis*, which correspondingly lost the increased pathogenicity conferred by LRV1. These compounds hold promise as leads to ameliorate the severity of LRV1-bearing *Leishmania* infections, and raise the possibility of targeting other protozoal infections whose pathogenicity may be exacerbated by similar endogenous viruses.

Author contributions: F.M.K., N.F., and S.M.B. designed research; F.M.K., J.I.R., and C.R. performed research; G.R.B. contributed new reagents/analytic tools; F.M.K., J.I.R., C.R., and S.M.B. analyzed data; and F.M.K. and S.M.B. wrote the paper.

Reviewers: B.U., Oregon Health Sciences University; and C.C.W., University of California, San Francisco.

The authors declare no conflict of interest.

[1]To whom correspondence should be addressed. Email: stephen.beverley@wustl.edu.

This article contains supporting information online at www.pnas.org/lookup/suppl/doi:10.1073/pnas.1619114114/-/DCSupplemental.

microbial sources including the microbiota or coinfections (23). Recent studies show that the presence of LRV1 in clinical isolates of *L. braziliensis* and *L. guyanensis* correlates with drug-treatment failure (17, 20), phenomena that could readily be explained by the increased parasite numbers or altered host responses predicted from animal models (7, 13, 24). Thus, current data support a role for LRV1 in increasing disease severity in human leishmaniasis (13); this suggests that therapies targeting LRV1 specifically could be applied toward amelioration of disease pathology. As one approach, murine vaccination using the LRV1 capsid results in significant protection against LRV1$^+$ *L. guyanensis* (25).

Here we describe a complementary approach, targeting LRV1 directly using small-molecule inhibitors. Although effective antivirals are available for many viral targets including retroviruses, DNA viruses, and single-strand RNA (ssRNA) viruses (26), little effort has gone into agents acting against dsRNA viruses (27). These comprise at least 10 viral families (Birnaviridae, Botybirndaviridae, Chrysoviridae, Cystoviridae, Megabirnavirdae, Partitiviridae, Picobirnaviridae, Quadriviridae, Reoviridae, and Totiviridae), infecting a wide array of hosts, including fungi, plants, and animals (28). Some constitute important agricultural pathogens and rotaviruses (Reoviridae) cause serious human disease. For protozoan viruses, their role in the exacerbation of human disease is only now beginning to be appreciated (6, 29). Because viral elements are critical factors acting to exacerbate the disease where studied, candidate anti-LRV1 agents should be viewed as "antipathogenicity" treatments rather than sterilizing cures (30), which could be used alone or more likely in combination with existing antileishmanial agents in the treatment of ongoing infection.

As a starting point, we focused on nucleoside analogs, a class that includes many widely used and effective antivirals (Table S1) (26). Following uptake and activation to the triphosphate form, these analogs primarily target viral replication, with different classes acting preferentially against viral DNA or RNA polymerases (RDRP) or reverse transcriptases, as well as cellular metabolism. A second rationale was that *Leishmania* are purine auxotrophs, with highly active and multiply redundant pathways for uptake and activation of nucleobases and nucleosides (31). Indeed, a great deal of prior effort has been devoted to the development of antileishmanial purine analogs; however, whereas the nucleobase allopurinol is commonly used as a veterinary agent, it has proven more difficult to find agents of sufficient potency and selectivity against *Leishmania* to be used widely against human leishmaniasis (32). We reasoned that the highly divergent properties of Totiviridae RDRPs, relative to the polymerases of both the *Leishmania* and mammalian hosts (as well as other viral RDRPs), could prove fertile grounds for antiviral discovery, especially when coupled with potentiation by the parasite's powerful nucleoside/base salvage pathways.

Results

Measurement of LRV1 Levels by Capsid Flow Cytometry. Because LRV1 (like most Totiviridae) is not shed from the cell (33, 34), we developed a flow cytometric assay to measure intracellular LRV1 capsid levels on a per cell basis. To detect LRV1 we used binding to a rabbit anti-*Lgy*LRV1 capsid antiserum (35) followed by detection with Alexa Fluor488-conjugated goat anti-rabbit IgG. We found that fixation with 2% (wt/vol) paraformaldehyde followed by permeabilization with Triton X-100 yielded a clear LRV1-dependent profile (Fig. 1*A*). Titration of the anticapsid antiserum showed that dilutions around 1:16,000 gave a strong signal with excellent selectivity between *Lgy*LRV1$^+$ and LRV1$^-$ (Fig. 1*B*), with little background staining evident in immunofluorescence microscopy. Under these conditions and as seen in previous immunofluorescence studies (36), *Lgy*LRV1$^+$ showed a strong, homogeneous LRV1 distribution (Fig. 1*A*). We attempted similar studies with anti-dsRNA antibodies (36), but were unable to identify fixation conditions that gave similarly clear discrimination between *Lgy*LRV1$^+$ and LRV1$^-$ by flow cytometry.

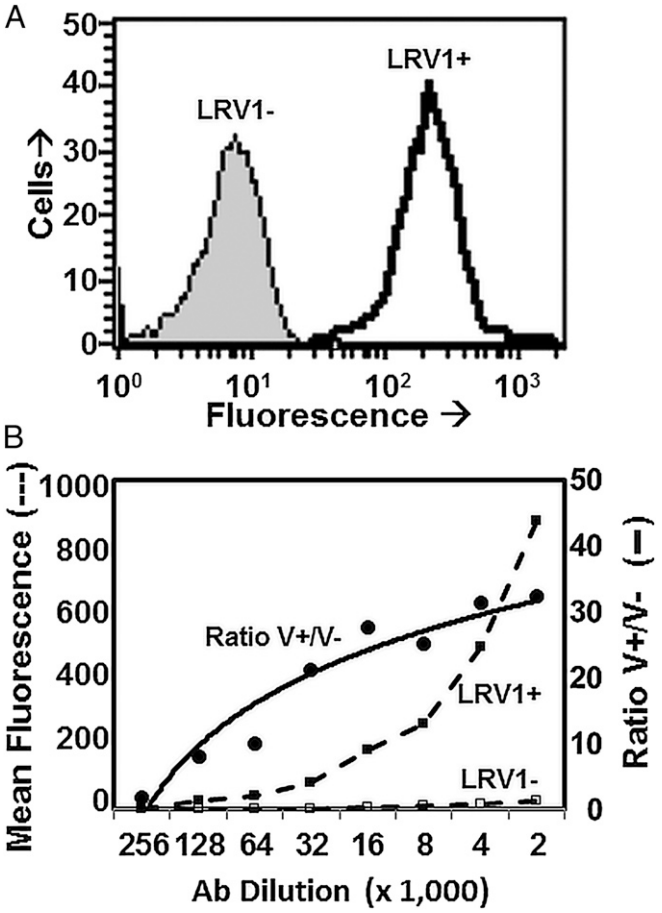

Fig. 1. Anti-LRV1 capsid flow cytometry. *Lgy*LRV1$^+$ and *Lgy*LRV1$^-$ parasites were fixed and permeabilized followed by staining with increasing dilutions of anticapsid antibody and fluoresceinated secondary antibody. (*A*) Profiles obtained with *Lgy*LRV1$^+$ (solid line) and *Lgy*LRV1$^-$ (filled) after selection for single cells. A representative experiment is shown, performed at a dilution of 1:16,000; subsequent studies were performed using a dilution of 1:20,000 ($n > 11$). (*B*) Mean fluorescence of *Lgy*LRV1$^+$ (■) and *Lgy*LRV1$^-$ (□) for each antibody dilution. The ratio of LRV1$^+$/LRV1$^-$ staining (●) is plotted as a solid line.

Inhibition Tests. We acquired a collection of 81 compounds, primarily nucleoside or nucleobase analogs, including ones shown previously to be active against diverse viruses, tumor cells, or *Leishmania* (Fig. S1 and Tables S1 and S2). These compounds were examined for their ability to inhibit the growth of *Lgy*LRV1$^+$ and virus levels by LRV1 capsid flow cytometry. *Lgy*LRV1$^-$ parasites grew similarly to *Lgy*LRV1$^+$ and were used as virus-negative controls. These data revealed three patterns (Fig. 2). For most compounds, LRV1 capsid levels were not significantly affected, within a factor of ~3 (Fig. 2, black or red dots within large dashed gray and red circles, Fig. S2, and Table S2). All nucleobase analogs fell within this group, as did foscarnet (a structure analog of pyrophosphate). Within this group, a subset showed more than 10-fold inhibition of *L. guyanensis* growth (Fig. 2, red dashed circle and black dots above; Fig. S3 *A* and *B*; and Table S2), including known antileishmanials, such as allopurinol, mycophenolic acid, and 4-aminopyrazolopyrimidine (APP). Several additional compounds showed leishmanial inhibition at the concentration tested (Fig. 2, Fig. S2*B*, and Table S2); however, these were deprioritized for various reasons, including known mammalian cell toxicity. In the initial screens several compounds showed modest elevation of

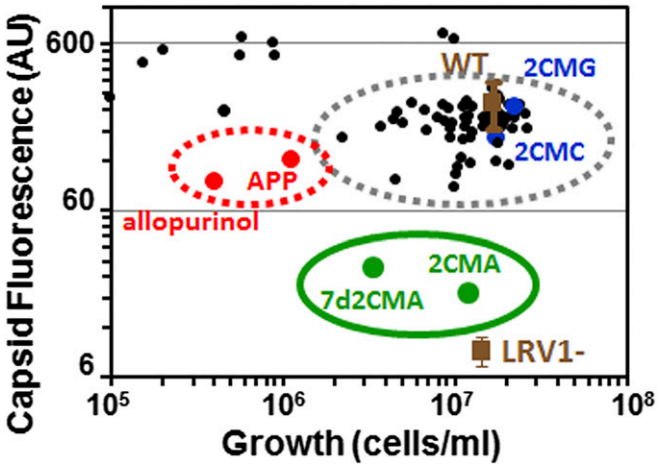

Fig. 2. Antiviral inhibition of *L. guyanensis* growth vs. LRV1 inhibition. The figure shows data from Table S2 plotted; LRV1 capsid levels (*y* axis) vs. *L. guyanensis* growth (*x* axis). The large dashed gray circle marks compounds (black dots) showing little effect on LRV1 or *L. guyanensis*, the red circle marks compounds preferentially inhibiting *L. guyanensis* growth, and the green circle marks compounds preferentially inhibiting LRV1; blue dots depict 2′C substituted nucleosides without anti-LRV1 activity. *Lgy*LRV1$^+$ and *Lgy*LRV1$^-$ controls are shown in brown. Abbreviations for compounds discussed further in the text can be found in Table S1.

LRV1, often accompanied by growth inhibition (Fig. 2, Fig. S2*A*, and Table S2). However, this effect was not always reproducible and was not pursued further.

Two compounds strongly reduced LRV1 capsid levels with minimal impact on parasite growth (Fig. 2, green circle, Fig. S1 and Table S2). Both 2′-C-methyladenosine (2CMA) and 7-deaza-2′-C-methyladenosine (7d2CMA) resulted in 12-fold reductions in LRV1 capsid levels, showing 30% and 90% inhibition of parasite density, respectively, when tested at 100 μM. Both had previously been shown to inhibit the hepatitis C virus (HCV) RDRP following activation (37, 38). In contrast, 2′-C-methylcytidine or guanosine had little effect on LRV1 levels or *L. guyanensis* growth (Fig. 2, blue dots). Compounds bearing a variety of other 2′ modifications (alone or in combination, with various bases) showed little effect on LRV1. These included sofosbuvir and mericitabine (related to 2′-C-methyl-2′-F uridine or cytidine, respectively), both of which show strong activity against HCV (39, 40), or NITD008, which shows good activity against flaviviruses (41). These data suggest a strong preference for both the nature of the 2′-C substitution, as well as adenine as the base. Note that these data cannot discriminate between effects arising from direct inhibition of RDRP or other viral processes, nor drug metabolism (phosphorylation or resistance to nucleoside hydrolases).

Previously, a *Leishmania* cysteine proteinase activity was implicated in the cleavage of the LRV1 capsid–RDRP fusion protein, potentially important for LRV1 biogenesis (42). However, no effects on *L. guyanensis* growth and only minimal effects on LRV1 capsid levels were observed with three cysteine proteinase inhibitors tested (E64, E64d, and CA-074) (Table S2), relative to the effects of 2CMA or 7d2CMA.

2CMA Preferentially Inhibits LRV1 Replication. Titrations were performed to quantitate the potency of 2CMA and 7d2CMA against *L. guyanensis* growth and LRV1, measuring the relative cellular growth rate to better assess fitness effects. For 2CMA, the EC_{50} was estimated to be ∼3 μM for LRV1 capsid inhibition, versus >100 μM for parasite growth (Fig. 3*A*), at least 30-fold selective. To assess the effects on replication of the dsRNA LRV1 genome directly, we used quantitative anti-dsRNA slot blots (Fig. 3*A*) (36), which showed an EC_{50} of ∼1 μM, slightly less than seen with capsid inhibition and consistent with the anticipated targeting of the RDRP. With 7d2CMA, an EC_{50} of ∼5 μM was seen against LRV1 capsid expression, versus ∼ >100 μM for *L. guyanensis* growth, again with about >20-fold selectivity (Fig. 3*B*). Several studies were carried out with *L. braziliensis* strains bearing LRV1 (12). The 2CMA EC_{50} for *Lbr*LRV1 was similar to that seen with *Lgy*LRV1 (∼3 μM); however, parasites were somewhat more susceptible to growth in inhibition (EC_{50} 50–100 μM). Because the available quantities of 7d2CMA were limiting and both compounds were similarly selective for *L. guyanensis*, we focused thereafter on 2CMA.

Inhibition of 2CMA LRV1 Is Unaffected by Exogenous Adenine, nor Is Synergy Seen with Antileishmanial Nucleobases. We asked whether the 2CMA potency was affected by the presence of exogenous adenine, present at about 5–33 μM in the yeast extract component of Schneider's medium (43). The addition of adenine up to 400 μM had no impact on LRV1 inhibition by 100 μM 2CMA, nor did it alter LRV1 levels in *Lgy*LRV1$^+$ (Fig. S3*C*). APP showed similar inhibition of *L. guyanensis* growth and LRV1 levels, whereas at the highest concentration tested, allopurinol inhibited *L. guyanensis* growth or LRV1 capsid levels by 30 or 60%, respectively (Fig. S3*A*). We then explored potential interactions between 2CMA and antileishmanial nucleobases. However, no change in the EC_{50} for 2CMA inhibition of *L. guyanensis* growth or LRV1 capsid synthesis was seen with increasing concentrations of allopurinol (∼3 μM) (Fig. S3*D*).

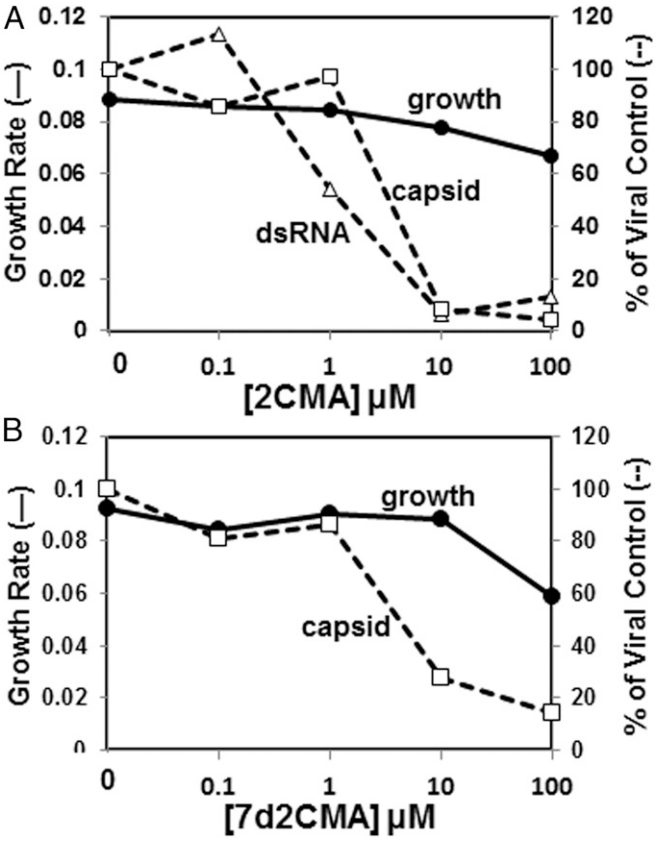

Fig. 3. 2CMA and 7d2CMA inhibition of *L. guyanensis* growth and LRV1 capsid or RNA levels. The figure shows the rate of growth or LRV1 capsid levels (*y* axis) as a function of drug concentration. (*A*) 2CMA; (*B*) 7d2CMA. Growth rate (●, solid line) and normalized LRV1 capsid (□, dashed line) or RNA (Δ, dashed line) are shown. The results of one representative experiment are shown for 2CMA ($n = 2$ for RNA and capsid) and a single experiment for 7d2CMA.

LRV1 Inhibition Is Independent of *Leishmania* Growth Inhibition. Agents inducing stress or growth arrest have been used to cure fungal Totiviridae, with cycloheximide (CHX) used often (44, 45). Growth of *L. guyanensis* at 10 or 100 nM CHX resulted in an increase in population doubling time, from ∼7.7 h to 11.2 or 44.7 h, respectively, without significant cell death as evidenced by resumption of WT growth following CHX removal (Fig. 4*A*). Despite the strong effects on growth, LRV1 capsid levels were unaffected, nor was the emergence of a "LRV1^{-}" parasite population seen at any CHX concentration (Figs. 4 *B* and *C*). Similar results were obtained with clotrimazole, which inhibits *Leishmania* growth through inhibition of sterol synthesis (Fig. 4*D*). Finally, no correlation was seen between LRV1 levels and growth rate in our test compound screening (Fig. 2 and Fig. S2) or exposure to hygromycin B (46). Thus, inhibition of *Leishmania* growth alone does not alter LRV1 levels.

Viral Loss Occurs by Random Dilution. The availability of an inhibitor with strong selectivity for LRV1 over parasite growth provided an opportunity to test the assumption that cytosolic Totiviruses are passed randomly to daughter cells during mitosis (34, 47). For maximal LRV1 inhibition, parasites were inoculated into 100 μM 2CMA, which increased the population doubling time from 6.4 to 8.5 h (Fig. 3). The average LRV1 levels immediately declined, with capsid and RNA levels falling in parallel (Fig. 5 *A* and *B*). Importantly, when plotted as a function of number of cell divisions, loss of LRV1 capsid and RNA followed a first-order linear relationship, with a 50% loss at every doubling (Fig. 5 *A* and *B*). When visualized at the population level by flow cytometry, LRV1 capsid levels per cell declined homogeneously at every time point tested until only background staining was evident by six cell doublings (Fig. 5*C*). Both of these observations closely match the expectation for the random distribution of LRV1 particles to daughter cells during mitosis and successive cell divisions.

2CMA Induces LRV1^{-} Populations. To explore the loss of LRV1 further, we performed a series of "washout" experiments, growing *Lgy*LRV1^{+} in 100 μM 2CMA for one, three, four, or six cell doublings followed by transfer to drug-free media. After one doubling, a time when LRV1 levels had only decreased twofold, LRV1 capsid levels rapidly returned to WT levels and distribution. In contrast, when 2CMA was maintained for three or four cell doublings, resulting in a homogeneous population showing on average 8- or 16-fold less LRV1 capsid expression, the washout lines now showed two distinct populations (Fig. 5 *C* and *D*). One population expressed LRV1 at levels similar to control *Lgy*LRV1^{+}, whereas the other resembled *Lgy*LRV1^{-} (Fig. 5*D*, *Top* and *Middle*). Parasites with *Lgy*LRV1^{+} capsid levels were the majority (55%) in the three-doubling washout population, whereas these had declined to 36% percent in the four-doubling washout population (Fig. 5*D*). The *Lgy*LRV1^{-} population increased from 31 to 50% of the total cell population during this time. Finally, after six cell doublings of growth with 2CMA, the LRV1 capsid profile was indistinguishable from that of the *Lgy*LRV1^{-} and the six-doubling washout population revealed only parasites maintaining the *Lgy*LRV1^{-} capsid-staining profile (Fig. 5*D*). This population was maintained for at least six passages (∼40 cell doublings) without return of any demonstrable LRV1^{+} parasites.

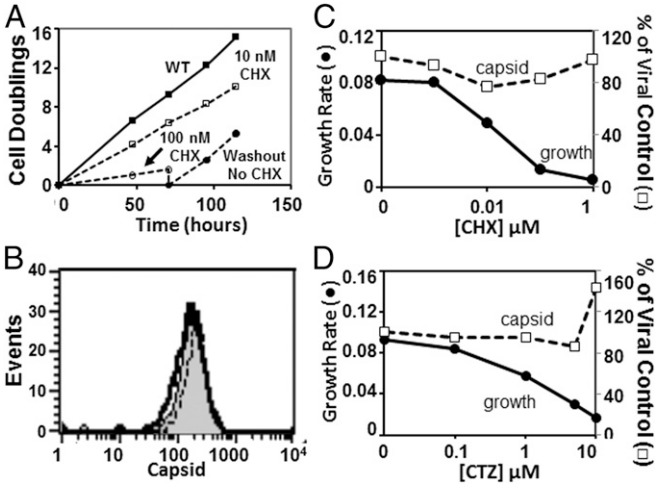

Fig. 4. LRV1 levels are unaffected by agents inhibiting *L. guyanensis* growth. (*A*) *Lgy*LRV1^{+} was treated with 10 nM CHX (□, dashed line), 100 nM CHX (○, dashed line), or no treatment (■, solid line). After 72 h, cells treated with 100 nM CHX were placed into fresh media (●, dashed line). (*B*) Profiles obtained by LRV1 flow cytometry after 48 h growth for WT (shaded) or cells treated with 100 μM CHX (solid line), or 10 μM CHX (dashed line). (*C*) Plot of growth rate of *Lgy*LRV1^{+} (●) or LRV1 capsid levels (□, dashed line) after 48-h propagation in increasing concentrations of CHX. (*D*) As in *C* but for clotrimazole (CTZ). A representative experiment is shown ($n = 3$).

Several conclusions emerge from these studies: first, the effective LRV1 copy number per cell must be relatively low, as otherwise an LRV1^{-} population could not emerge after only three to six cell doublings (Fig. 5), roughly corresponding to copy numbers of 8–64 ($2^3 - 2^6$) and consistent with fraction of LRV1^{-} cells emerging in the washouts (Fig. 5*D*). *Lgy*LRV1 copy number was previously estimated as 24–100 by competitive PCR assay (48). To assess LRV1 copy number independently in the clonal *Lgy*LRV1^{+} line studied here, we isolated total RNA quantitatively from a known number of cells, and estimated LRV1 copy number by quantitative RT-PCR (qRT-PCR), using a standard curve established from a cloned LRV1 genome (*Methods*). This process yielded an estimated average LRV1 copy number of 15 ± 0.9 per cell ($n = 3$), consistent with range estimated from the rate of drug-induced loss above.

Second, after washout, 2CMA-treated parasites, which originally showed homogeneous low levels of LRV1, now reverted to biphasic populations showing WT or "negative" LRV1 levels. The recovery of the WT-like population suggests that there may be a "set point" for LRV1 levels. Because only populations but not clones were studied, we cannot be sure that this occurred intracellularly; however, the rapidity with which LRV1 levels rebounded suggests this may be more likely.

Rapid Recovery of Matched Clonal WT and LRV1-Cured Lines. Our findings suggested that it should be relatively easy to recover LRV1^{-} clonal lines from the 2CMA-treated population. However, we were concerned that despite small effects on growth, the relatively high concentration of 2CMA used above could itself have unwanted selective effects on *L. guyanensis*. Support for this concern arose when in pilot studies, several clonal lines obtained after growth in 100 μM 2CMA lacked LRV1 but showed decreased growth inhibition by 2CMA. Thus, we repeated the LRV1 cure using 10 μM 2CMA, a concentration showing less of an effect on parasite growth but retaining strong inhibition of LRV1 levels (Fig. 3). Again, loss of LRV1 proceeded homogeneously (Fig. 6*A*). When clonal lines were recovered directly by plating from this population, very few were LRV1^{-} (1 of 30). However, if the population was allowed to grow in the absence of 2CMA for another ∼six cell doublings (washout), a bimodal population for LRV1 capsid levels emerged, as seen previously. Analysis of 12 clonal lines obtained by direct plating from this washout population showed that six exhibited LRV1 capsid levels/profiles identical to the *Lgy*LRV1^{-} control, whereas two showed profiles identical to the *Lgy*LRV1^{+} parent (representatives shown in Fig. 6*B*). Interestingly, four lines showed more complex profiles, with populations showing range of intensities

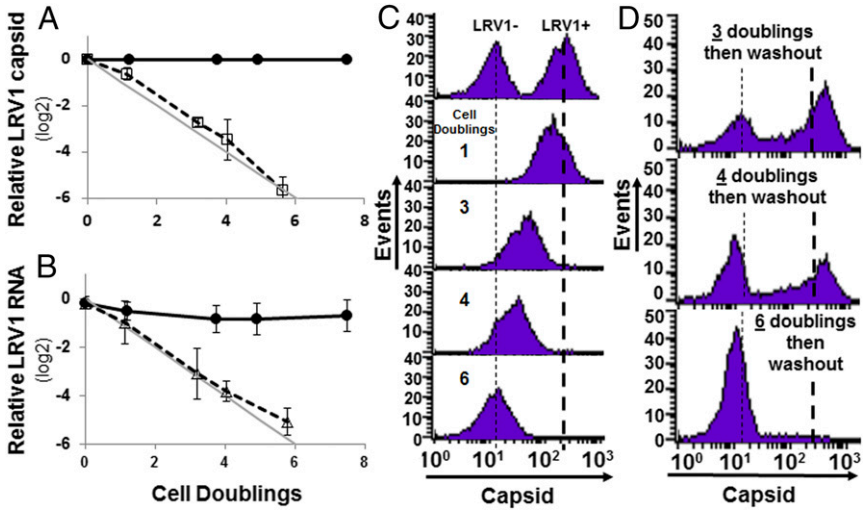

Fig. 5. Kinetics of and cellular distribution of LRV1 loss after treatment with 100 μM 2CMA. (*A* and *B*) *Lgy*LRV1$^+$ was inoculated into media without (●) or with (□, Δ) 100 μM 2CMA, and growth and LRV1 capsid (□, dashed line) and RNA levels (Δ, dashed line) measured by capsid flow cytometry (*A*) or qRT-PCR (*B*). For *A*, results at each time are shown normalized to LRV1$^+$ and LRV1$^-$ control levels using the formula $\log_2$ (2CMA treated − LRV1$^-$)/(LRV1$^+$ − LRV1$^-$). For *B*, the $\log_2$ ddCT values are shown. A theoretical 1:2 dilutional loss is shown (thin gray line); error bars represent ±1 SD. (*C*) LRV1 capsid flow cytometry of control parasites (*Top*) and populations grown for one, three, four, or six cell doublings in 100 μM 2CMA. (*D*) LRV1 capsid flow cytometry of parasites grown for three, four, or six doublings in 100 μM 2CMA, and then grown for an additional six cell doublings in drug-free media (washouts). Thick and thin gray dashed lines represent *Lgy*LRV1$^+$ and *Lgy*LRV1$^-$, respectively.

spanning those from LRV1$^-$ to LRV1$^+$ controls (representative shown in Fig. 6*B*). These complex lines were not studied further. The set-point hypothesis predicts that upon further growth, those lines would ultimately revert to bimodal populations.

We chose two LRV1$^+$ and LRV1-cured lines that had experienced identical 2CMA treatment and culture manipulations. Growth tests confirmed these were not resistant to 2CMA, and RT-PCR and Western blot tests confirmed the presence or absence of LRV1 (Fig. 6 *C* and *D*). These clones thus constituted matched WT and LRV1-cured lines appropriate for subsequent studies of LRV1 effects.

LRV1 Correlates with Increased Cytokine Secretion and Mouse Infectivity. With matched 2CMA-treated LRV1$^+$ and LRV1$^-$ (cured) lines, we asked whether LRV1 was correlated with elevated pathology and hyperinflammatory responses, as expected (7, 12). Infections were performed with bone marrow-derived macrophages (BMM) in vitro, followed by assays for secretion of two characteristic LRV1-dependent cytokine reporters, IL-6 and TNF-α. Cytokine secretion induced by the LRV1$^+$/2CMA-treated lines was comparable to that of the parental *Lgy*LRV1$^+$ line, whereas cytokine secretion induced by the 2CMA cured lines was considerably less, and comparable to that of the *Lgy*LRV1$^-$ control (Fig. 7 *A* and *B*).

Infections of susceptible BALB/c mice were performed followed by measurement of pathology (footpad swelling) and bioluminescent imaging of parasite numbers. A strong LRV1-dependency for both pathology and parasite abundance was observed in comparisons of the matched 2CMA-treated LRV1$^+$ vs. LRV1$^-$ (cured) lines (Fig. 7 *C* and *D*). Importantly, the response to the 2CMA-treated LRV1$^+$ lines closely matches that to the control parental *Lgy*LRV1$^+$ line and, similarly, the response to the 2CMA-treated LRV1$^-$ line closely matches that to the *Lgy*LRV1$^-$ control (Fig. 7 *C* and *D*), both of which were studied previously (7).

Discussion

In this study, we report the identification of compounds specifically targeting the LRV1 dsRNA virus of *L. guyanensis* and *L. braziliensis*, two representatives of the Totiviridae. Our findings have relevance for the specific therapeutic inhibition of *Leishmaniavirus*, basic studies of viruses within the Totiviridae, the development of antivirals directed against dsRNA viruses generally, and the development of new tools for assessing the role of LRV1 in elevating *Leishmania* pathogenicity.

To facilitate the search for LRV1 inhibitors, we first developed a capsid flow cytometry assay to rapidly monitor LRV1 capsid levels (Fig. 1). This assay can be performed in only a few hours, and although these studies used it in a relatively low throughput manner, it should be scalable for higher throughput. The results were confirmed by anticapsid or anti-dsRNA Western or slot blotting, or quantitative RT-PCR (Fig. 6 *C* and *D*). Additionally, this assay provides useful information about the cellular heterogeneity of LRV1 levels not readily achievable by other methods, which informed studies probing the inheritance of LRV1 as well as in the generation of LRV1$^-$ lines.

We focused on known antivirals for several reasons: first, despite significant advances in targeting many retroviruses, DNA viruses, or ssRNA viruses, very little effort or progress has been devoted on inhibition of dsRNA viruses. Thus, there seemed a reasonable potential for "repurposing" known antivirals against the dsRNA *Leishmaniavirus.* Moreover, because many antivirals are nucleoside analogs and that *Leishmania* is a purine auxotroph (31), the pharmacokinetics of drug uptake and metabolism could well favor the efficacy of such compounds against *Leishmaniavirus*. As a collateral benefit, these studies had the potential to uncover new lead inhibitors against *Leishmania* itself, as auxotrophy has prompted many investigators to target purine metabolism for antileishmanial therapy. Several new compounds not previously reported to inhibit *Leishmania* were identified (Fig. 2 and Tables S1 and S2), but were not pursued further here.

We identified two compounds that showed preferential inhibition of LRV1, 2CMA, or 72CMA (Fig. 3 and Fig. S1). The two active compounds were effective in the micromolar range, with >20-fold selectivity for LRV1 versus *L. guyanensis* growth inhibition and were also active against *Lbr*LRV1, albeit with somewhat less selectivity over growth. The EC_{50} measured using dsRNA or capsid levels were similar, with that of the dsRNA being somewhat less, consistent with the anticipated mode of action targeting the RDRP and genome replication. Both compounds have demonstrated

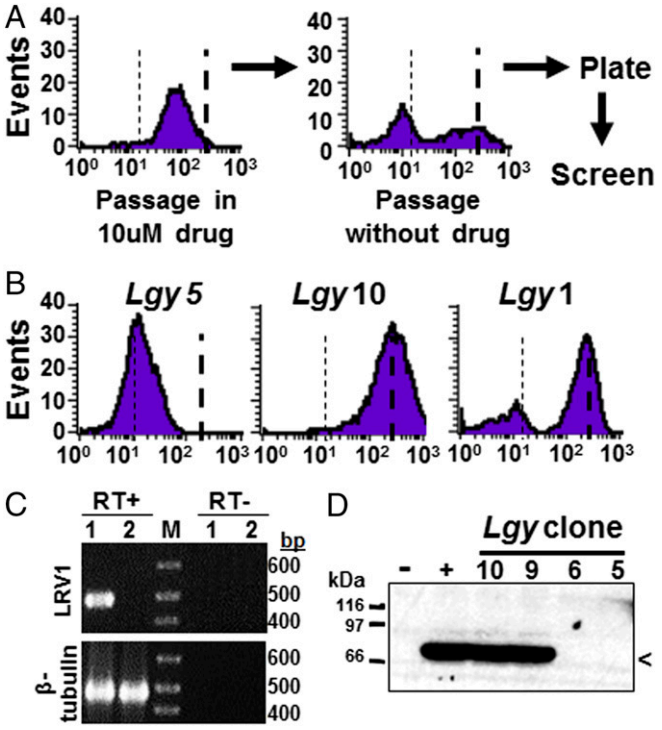

Fig. 6. Generation of matched LRV1$^+$and cured lines after limited 10 μM 2CMA treatment. (*A*) Workflow for treatment of parasites with 10 μM 2CMA before isolation of clonal lines. First drug treatment for 6.4 cell doublings generates a population containing low average LRV1 levels, then the washout for 6 cell doublings allows resolution into fully negative or LRV1$^+$ lines. (*B*) Representative LRV1 capsid profiles for a cured line (*L. guyanensis* clone 10-5), a WT-like line (*L. guyanensis* clone 10-10), and a mixed profile line (*L. guyanensis* clone 10-1; for clarity the leading "10" is omitted from the figures). (*C*) RT-PCR tests confirming presence or absence of LRV1 in treated lines. RT+, reverse transcription performed before PCR; RT−, no reverse transcription step. M, 1 kb+ ladder, Invitrogen. The expected LRV1 capsid and β-tubulin amplicons of 496 and ∼450 nt were found. (*D*) Western blotting with anti-*Lgy*LRV1 capsid antisera confirms absence of LRV1 in cured lines *L. guyanensis* 10-5 and 10-6. M, molecular weight marker. The arrowhead marks the position of the 95-kDa LRV1 capsid band.

activity against HCV, where they target the viral RDRP by chain termination (37, 38, 49). By molecular modeling of the *L. guyanensis* LRV1 RDRP domain against other RDRPs, such as HCV, we were able to generate a view of the active site including residues putatively binding to the nucleotide substrates (Fig. S4). Notably, these included sites homologous to those mutated in HCV nucleoside analog-resistant lines (50). This finding supports our working hypothesis that both anti-LRV1 compounds are activated to triphosphates, where they act to inhibit RDRP activity. These compounds represent the only inhibitors known to act against any member of the Totiviridae, and indeed some of the few candidates described inhibiting dsRNA viruses generally.

Common features of the two selective anti-LRV1 compounds include the 2′-C methyl and the adenine base moieties, although 2′ C-methyl G and C were inactive against both *Leishmania* and LRV1. A similar pattern was observed for dengue virus RDRP inhibitors, where only adenosine analogs demonstrated antiviral activity (51). Following uptake, in *Leishmania* most purine nucleosides are metabolized to nucleobases, the major exception being adenosine, which is phosphorylated directly by adenosine kinase (31). This finding could contribute to the superiority of 2CMA analogs. However, all other 2′C-modified analogs tested failed to inhibit LRV1 or *Leishmania*, including ones bearing adenine or related moieties as the nucleobase (Fig. 2 and Tables S1 and S2). Other factors may include differential ability to be phosphorylated, often the rate-limiting step for antiviral nucleoside activation (52, 53), or susceptibility to nucleoside hydrolases or phosphorylases, which *Leishmania* possess in abundance (31), and affinity of the phosphorylated analog with the LRV1 RDRP itself. Additional studies will be required to assess the contributions of each of these factors to anti-LRV1 activity and the design of more potent inhibitors.

Anti-LRV1 Agents as a Tool for Studying *Leishmaniavirus* Replication and Biology. The LRV1 selectivity of 2CMA and 7d2CMA provided the foundation for several studies probing LRV1 biology. Under 2CMA inhibition, a first-order kinetic loss of LRV1 was observed, (measured by either capsid or dsRNA genome levels), with a homogeneous 50% loss at every cell doubling (Fig. 5 *A* and *B*). This finding fits exactly the prediction assumed by a random-inheritance model of LRV1 particles during mitosis. Although widely assumed for the inheritance of most persistent dsRNA viral infections, these findings now provide direct evidence of random segregation. These data also provide a mechanistic explanation for the failure to identify compounds inhibiting both LRV1 and *L. guyanensis* in our screen, because without continued parasite growth LRV1 cannot be lost by dilution, and indeed may increase somewhat (Fig. 2).

Ultimately, LRV1 levels declined to levels approaching those of LRV-free parasites within three to six cell doublings following 2CMA treatment (Fig. 5). This finding implies the viral copy number was relatively low, less than 8–64 (2^{3-6}), significantly less than previous estimates of 120 for *Lgy*LRV1 and often many thousands for other Totiviridae (34, 48). However, quantitative analysis of cellular LRV1 and total RNA led to an estimate of about 15, consistent with estimates of LRV1 abundance from recent whole-genome RNA sequencing by our group. If this unexpectedly low value for LRV1 copy number applies generally to LRV1s in other *Leishmania* strains or species, it could provide

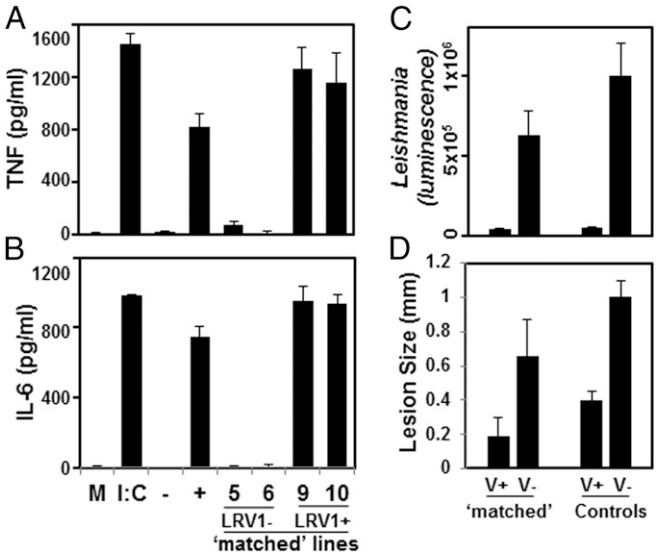

Fig. 7. Matched 2CMA-treated LRV1$^+$ and LRV1$^-$ cured lines recapitulate LRV1-dependent virulence. (*A* and *B*) Cytokine secretion by BMM infected 24 h after infection with *L. guyanensis* lines or treatment with poly I:C (2 μg/mL), M, media. (*A*) TNF-α; (*B*) IL-6. The figure shown is representative of three experiments, each done in triplicate; error bars represent ± SD. (*C* and *D*) Infections of matched 10 μM 2CMA treated *Lgy*LRV1$^+$ and *Lgy*LRV1$^-$. Parasite numbers (luminescence from luciferase reporter) (*C*) or footpad swelling (*D*) was measured at the peak of the infection (28 d). Each bar represents pooled data from eight mice total, four for each *Lgy* line used. LRV1$^+$ (clones 10-9 and 10-10) and LRV1$^-$ (clones 10-5 and 10-6) lines are shown; error bars represent ± SD. Data for control parasites are replotted from Ives et al. (7).

a new perspective on the observation that thus far, no images of LRV1 in situ by electron microscopy appear in the literature.

The rapid decline of LRV1 following 2CMA treatment suggested that it would be relatively easy to recover LRV1-free clonal lines. Following washout of 2CMA after three to six cell doublings and a brief period of growth without drug, cultures manifested two distinct parasite populations by capsid flow cytometry: one similar to *Lgy*LRV1$^+$ and a second similar to *Lgy*LRV1$^-$ (Figs. 5 and 6). The fraction of *Lgy*LRV1$^-$ parasites grew progressively with increasing 2CMA treatment, reaching levels approaching 100%. To recover parasites suited for studies focusing on the biological properties of LRV1$^-$ parasites, we adopted a protocol in which parasites were treated for only a brief period with 10 μM 2CMA, a concentration showing little effect on parasite growth but relatively high inhibition of LRV1 (Fig. 3), followed by brief passaging and then plating on drug-free media. Importantly, this procedure allowed the recovery of both LRV1$^+$ and LRV1$^-$ matched clonal lines, which had experienced identical treatment, thereby facilitating comparisons probing LRV1 effects (below). Interestingly, in all of these studies the LRV1 levels in washout lines showed a strong tendency to recover from the low levels seen in drug to those comparable to LRV1$^+$ controls (Fig. 5). These findings suggest that the LRV1 copy number is maintained at a specific set point, perhaps through a balance between replication and the RNAi pathway (12, 54). Previous studies examining LRV1 transcripts during growth phase also concluded that LRV1 copy number is regulated (48).

For other fungal dsRNA viruses, treatments engendering cell stress or growth inhibition have been used to generate virus-free lines at significant frequencies, one common example being the use of CHX to cure the yeast L-A virus (44). Although in one prior study LRV1 cure was obtained during a series of transfection and hygromycin selection steps, this appears to have been successful only once, and our laboratories have been unable to repeat this (12, 46). Here we were unable to show any correlation between LRV1 loss and drug-induced stress or growth inhibition with CHX, the ergosterol synthesis inhibitor clotrimazole, or within the large panel of test compounds (Figs. 2 and 4, Fig. S2, and Tables S1 and S2). Thus, LRV1 appears to be relatively stable to growth inhibitory stresses. However, given its relatively low cellular copy number (<20), on a strictly probabilistic basis LRV1$^-$ variants might occur at a low frequency, which occasionally may emerge or be recovered by methods more sensitive than used here.

Antiviral Cures and the Generation of Isogenic LRV1$^-$ Lines for the Study of LRV1-Dependent Virulence. Treatment with 2CMA enables the controlled and reproducible generation of matched LRV1$^+$ and LRV1-cured lines without difficulty. In vivo, 2CMA-cured LRV1$^-$ parasites showed less pathology and lower parasite numbers and induced less cytokine secretion than LRV1$^+$ parasites, comparable to the single spontaneous LRV1$^-$ lines described previously (Fig. 7). Thus, our LRV1 toolkit now includes two independent, reproducible, and efficient methods for generating isogenic LRV1$^-$ lines, which will facilitate tests probing the biology of LRV1-dependent pathogenicity in diverse parasite backgrounds. Depending on the relative selectivity of the antivirals and the presence of an RNAi pathway, one method may be superior for a given *Leishmania* species or strain.

The Potential for Antitotiviral Therapy in the Treatment of dsRNA-Bearing Parasites and Disease. There are now ample data suggesting that LRV1 contributes to the severity in human leishmaniasis (6, 13, 17, 19, 20, 55), suggesting that anti-LRV1 inhibitors could be clinically useful, alone or in conjunction with existing antileishmanials. Unfortunately, pharmacokinetic studies of the two compounds studied here in mammals suggest that neither of these are good candidates for testing of this hypothesis just yet, as the concentration needed for LRV1 elimination (10 μM) is above the maximum achievable serum concentration in various mammalian models, typically less than 1 μM (38, 49, 56). Thus, future efforts must focus on the development of compounds with higher potency targeting LRV1, without significant human host toxicity. For therapeutic purposes a compound simultaneously targeting both would likely be superior. However, because *Leishmania* growth is required for LRV1 to be lost by progressive dilution (Fig. 5), a screening method different from that used here will be required to detect such agents. Dilutional loss following anti-LRV1 inhibitor treatment in vitro predicts that very low levels of LRV1 could persist after treatment in vivo, whether measured on a total or per cell basis (Fig. 5). Importantly, previous data show that below a certain threshold, parasites bearing low LRV1 levels are controlled as effectively as LRV1$^-$ lines (7).

Our studies also raise the possibility of treating other diseases caused by protozoans bearing dsRNA viruses, which show endogenous virus-dependent pathogenicity, including Totiviridae present within *Trichomonas vaginalis* (*Trichomonasvirus*), *Giardia lamblia* (*Giardiavirus*), or *Eimeria* (*Eimeravirus*) (34, 57), and Partitiviridae within *Cryptosporidium parvum* (*Cryspovirus*) (58, 59). Potentially, agents targeting these putative pathogenicity factor viruses could prove similarly valuable for laboratory studies of these viruses as well.

Methods

Parasites and Growth Media. Most studies were performed using luciferase-expressing transfectants of *L. guyanensis* (MHOM/BR/78/M4147) described previously [LRV1$^+$ *Lgy*M4147/SSU:IR2SAT-LUC(b)c3 and LRV$^-$ *Lgy*M4147/pX63HYG/SSU:IR2SAT-LUC(b)c4] (54); these lines are termed *Lgy*LRV1$^+$ and *Lgy*LRV1$^-$, respectively. Two strains of LRV1$^+$ *L. braziliensis* were examined: LEM2780 (MHOM/BO/90/CS) and LEM3874 (MHOM/BO/99/IMT252 no. 3) (12). Parasites were grown in Schneider's media (Sigma) prepared according to the supplier's instructions with pH adjusted to 6.5 and supplemented with 0.76 mM hemin, 2 μg/mL biopterin, 50 U/mL penicillin, 50 μg/mL streptomycin, and 10% (vol/vol) heat-inactivated FBS. Cell concentrations were determined using a Coulter Counter (Becton Dickinson).

Drug-Inhibition Tests. Compounds were purchased or obtained as summarized in Table S1, and the structures of the two most active anti-LRV1 compounds are shown in Fig. S1. Stock solutions were prepared as recommended by the source, typically in DMSO at 50 mM, and tested against parasites at 100 μM or the maximum concentration permitted by drug solubility (Table S2). Parasites were inoculated at 2×10^5 cells/mL into Schneider's media lacking supplemental adenine. Growth was evaluated after 2 d, before the controls reached stationary phase growth, at which time parasite numbers had increased nearly 100-fold. Experiments were performed in sets of 10 test compounds, along with LRV1$^+$ and negative controls; the agreement among independent experiments among the controls was excellent, and the results are shown averaged together across all experiments (Table S2).

LRV1 Capsid Flow Cytometry. For capsid flow cytometry, 10^7 cells were fixed at room temperature using 2% (wt/vol) paraformaldehyde (Thermo Fisher) in PBS for 2 min. They were then incubated in blocking buffer [10% (vol/vol) normal goat serum (Vector Laboratories) and 0.2% Triton X-100 in PBS] for 30 min at room temperature. Anti-*Lgy*LRV1 capsid antibody (35) was added (1:20,000 dilution) and incubated at room temperature for 1 h. After two washes with PBS, cells were resuspended in in 200 μL PBS with Alexa Fluor488-labeled goat anti-rabbit IgG (Alexafluor, Invitrogen; 1:1,000; or Thermo Fisher; 1:2,000 dilution), and incubated 1 h at room temperature. After two additional washes with PBS, cells were subjected to flow cytometry, gating for single cells using forward and side scatter and the data analyzed using CellQuest software (BD Bioscience).

RNA Purification, cDNA Preparation, and qRT-PCR. For RNA purification, 10^7 cells were resuspended in 350 μL TRIzol Reagent and RNA was extracted using the Direct-zol RNA purification kit according to protocol (Zymo Research). RNA was then treated with DNase I (Ambion) for 1 h at 37 °C and repurified using RCC-5 column purification (Zymo Research). cDNA was prepared using SuperScript III (Invitrogen) and random priming according to protocol. RNA denaturation occurred at 65 °C for 5 min. RT-PCR tests were performed using LRV1-specific primers (SMB4647 5′-TBRTWGCRCACAGTGAYGAAGG and SMB4648 5′CWACCCARWACCABGGBGCCAT) or β-tubulin mRNA

(SMB5023 5′-AACGCTATATAAGTATCAGTTTCTGTACTTTA and SMB2110 5′-GACAGATCTCATCAAGCACGGAGTCGATCAGC). qRT-PCR was performed as previously described (36), with a 123-bp fragment of LRV1 capsid mRNA amplified with primers SMB5335 (5′-CTGACTGGACGGGGGGTAAT) and SMB5336 (5′-CAAAACACTCCCTTACGC), and a 100-bp fragment of KMP-11 (a *Leishmania* housekeeping gene) with primers SMB5548 (5′-GCCTGGATGAGGAGTTCAACA) and SMB5549 (5′-GTGCTCCTTCATCTCGGG). The reaction used Power SYBR Green (Applied Biosystems) in an ABI Prism 7000. Initial denaturation was at 95 °C for 10 min followed by 40 cycles of amplification with 15 s at 95 °C, and 1 min at 60 °C. Data were analyzed using ABI 7000 SDS software (v1.2.3) and normalized using the ΔΔCT method (60). RNA slot blot analysis was performed as described previously (36). The LRV1 copy number per cell was estimated in comparison with a standard curve generated using DNA from a plasmid bearing the LRV1 capsid gene (B6760, pBSKLRV1-4) and the average yield of RNA per cell across multiple *L. guyanensis* RNA preparations (5.12 ± 1.17 μg/10^7 cells; $n = 34$).

Isolation of LRV1$^+$ and LRV1$^-$ Clonal Lines by Brief Treatment with 2CMA. *Lgy*LRV1$^+$ parasites were grown for one passage in media containing 25 μg/mL nourseothricin (Werner BioAgent) to verify the presence of the integrated luciferase (LUC) gene (54). Cells were then grown one passage in the absence of nourseothricin, and inoculated into Schneider's media at a concentration of 2×10^5 cells/mL into media containing 10 μM 2CMA. Growth was measured and LRV1 quantitated by capsid flow cytometry. At various times, cells were either plated directly, or transferred to drug-free media, and allowed to grow an additional six cell doublings before plating. For both, the semisolid M199 media contained 50 μg/mL nourseothricin, and cells were diluted so that no more than ∼100 colonies were obtained per plate.

Macrophage Infections, Cytokine Assays, and Mouse Infection. Infections of C57BL/6 mouse bone marrow-derived macrophages and cytokine assays were performed as previously described (7, 10). Poly I:C was obtained from Invivogen and used at 2 μg/mL. For mouse infections, 5- to 6-wk-old C57BL/6 mice were purchased from Jackson Laboratories. Parasites were grown into stationary phase (2 full days) and 10^6 parasites were injected on the plantar aspect of the left foot. Measurement of footpad swelling was performed weekly using a Vernier caliper. Parasite numbers were assessed by luminescence of an integrated firefly luciferase reporter, measured using an IVIS 100 instrument as described previously (7, 54) and analyzed with Living Image software v2.60 (Perkin-Elmer).

Statement Identifying Institutional and Licensing Committee Approving Animal Experiments. Animal handling and experimental procedures were undertaken with strict adherence to ethical guidelines relevant in both host countries. These are set out by the Swiss Federal Veterinary Office and under inspection by the Department of Security and Environment of the State of Vaud, Switzerland. Experiments were carried out in strict accordance with the recommendations in the *Guide for the Care and Use of Laboratory Animals* of the National Institutes of Health (61). Animal studies were approved by the Animal Studies Committee at Washington University (protocol #20090086) in accordance with the Office of Laboratory Animal Welfare's guidelines and the Association for Assessment and Accreditation of Laboratory Animal Care International.

ACKNOWLEDGMENTS. We thank N. S. Akopyants, E. A. Brettmann, D. E. Dobson, L.-F. Lye, and S. Schlesinger for discussions and comments on this manuscript; Chantal Desponds, Florence Prevel, and Haroun Zangger for excellent technical assistance; and Jean Patterson (Texas Biomedical Research Institute) for providing capsid antisera. This work was supported by NIH Grants R01AI029646 and R56AI099364 (to S.M.B.); Fonds National de la Recherche Scientifique Grants 3100A0-116665/1 and IZRJZ3_164176/1 (to N.F.); Sigma-Aldrich Predoctoral and the Sondra Schlesinger Graduate Student fellowships (to J.I.R.); and the Division of Infectious Diseases (F.M.K.).

1. Alvar J, et al.; WHO Leishmaniasis Control Team (2012) Leishmaniasis worldwide and global estimates of its incidence. *PLoS One* 7(5):e35671.
2. Bañuls AL, et al. (2011) Clinical pleiomorphism in human leishmaniases, with special mention of asymptomatic infection. *Clin Microbiol Infect* 17(10):1451–1461.
3. Singh OP, Hasker E, Sacks D, Boelaert M, Sundar S (2014) Asymptomatic *Leishmania* infection: A new challenge for *Leishmania* control. *Clin Infect Dis* 58(10):1424–1429.
4. Pigott DM, et al. (2014) Global distribution maps of the leishmaniases. *eLife* 3:3.
5. WHO (2010) Control of the leishmaniases: WHO Expert Committee on the Control of Leishmaniases. World Health Organization Technical Report Series 949 (WHO, Geneva).
6. Hartley MA, Drexler S, Ronet C, Beverley SM, Fasel N (2014) The immunological, environmental, and phylogenetic perpetrators of metastatic leishmaniasis. *Trends Parasitol* 30(8):412–422.
7. Ives A, et al. (2011) *Leishmania* RNA virus controls the severity of mucocutaneous leishmaniasis. *Science* 331(6018):775–778.
8. Widmer G, Comeau AM, Furlong DB, Wirth DF, Patterson JL (1989) Characterization of a RNA virus from the parasite Leishmania. *Proc Natl Acad Sci USA* 86(15): 5979–5982.
9. Stuart KD, Weeks R, Guilbride L, Myler PJ (1992) Molecular organization of *Leishmania* RNA virus 1. *Proc Natl Acad Sci USA* 89(18):8596–8600.
10. Zangger H, et al. (2014) *Leishmania aethiopica* field isolates bearing an endosymbiontic dsRNA virus induce pro-inflammatory cytokine response. *PLoS Negl Trop Dis* 8(4):e2836.
11. Scheffter SM, Ro YT, Chung IK, Patterson JL (1995) The complete sequence of *Leishmania* RNA virus LRV2-1, a virus of an Old World parasite strain. *Virology* 212(1): 84–90.
12. Brettmann EA, et al. (2016) Tilting the balance between RNA interference and replication eradicates *Leishmania* RNA virus 1 and mitigates the inflammatory response. *Proc Natl Acad Sci USA* 113(43):11998–12005.
13. Hartley MA, et al. (2016) *Leishmaniavirus*-dependent metastatic leishmaniasis is prevented by blocking IL-17A. *PLoS Pathog* 12(9):e1005852.
14. Guerra JA, et al. (2011) Mucosal leishmaniasis caused by *Leishmania (Viannia) braziliensis* and *Leishmania (Viannia) guyanensis* in the Brazilian Amazon. *PLoS Negl Trop Dis* 5(3):e980.
15. Goto H, Lindoso JAL (2010) Current diagnosis and treatment of cutaneous and mucocutaneous leishmaniasis. *Expert Rev Anti Infect Ther* 8(4):419–433.
16. Mears ER, Modabber F, Don R, Johnson GE (2015) A review: The current in vivo models for the discovery and utility of new anti-leishmanial drugs targeting cutaneous leishmaniasis. *PLoS Negl Trop Dis* 9(9):e0003889.
17. Adaui V, et al. (2016) Association of the endobiont double-stranded RNA virus LRV1 with treatment failure for human leishmaniasis caused by *Leishmania braziliensis* in Peru and Bolivia. *J Infect Dis* 213(1):112–121.
18. Pereira LdeO, et al. (2013) Severity of tegumentary leishmaniasis is not exclusively associated with *Leishmania* RNA virus 1 infection in Brazil. *Mem Inst Oswaldo Cruz* 108(5):665–667.
19. Cantanhêde LM, et al. (2015) Further evidence of an association between the presence of *Leishmania* RNA virus 1 and the mucosal manifestations in tegumentary leishmaniasis patients. *PLoS Negl Trop Dis* 9(9):e0004079.
20. Bourreau E, et al. (2016) Presence of *Leishmania* RNA virus 1 in *Leishmania guyanensis* increases the risk of first-line treatment failure and symptomatic relapse. *J Infect Dis* 213(1):105–111.
21. Castellucci LC, et al. (2014) Host genetic factors in American cutaneous leishmaniasis: A critical appraisal of studies conducted in an endemic area of Brazil. *Mem Inst Oswaldo Cruz* 109(3):279–288.
22. Schriefer A, Wilson ME, Carvalho EM (2008) Recent developments leading toward a paradigm switch in the diagnostic and therapeutic approach to human leishmaniasis. *Curr Opin Infect Dis* 21(5):483–488.
23. Parmentier L, et al. (2016) Severe cutaneous leishmaniasis in a human immunodeficiency virus patient coinfected with *Leishmania braziliensis* and its endosymbiotic virus. *Am J Trop Med Hyg* 94(4):840–843.
24. Eren RO, et al. (2016) Mammalian innate immune response to a *Leishmania*-resident RNA virus increases macrophage survival to promote parasite persistence. *Cell Host Microbe* 20(3):318–328.
25. Castiglioni P, et al. (2016) Exacerbated leishmaniasis caused by a viral endosymbiont can be prevented by immunization with its viral capsid. *PLoS Negl Trop Dis* 11(1): e0005240.
26. De Clercq E, Li G (2016) Approved antiviral drugs over the past 50 years. *Clin Microbiol Rev* 29(3):695–747.
27. La Frazia S, et al. (2013) Thiazolides, a new class of antiviral agents effective against rotavirus infection, target viral morphogenesis, inhibiting viroplasm formation. *J Virol* 87(20):11096–11106.
28. King AMQ, Lefkowitz E, Adams MJ, Carstens EB (2011) *Virus Taxonomy: Ninth Report of the International Committee on Taxonomy of Viruses* (Elsevier, Amsterdam).
29. Fichorova RN, et al. (2012) Endobiont viruses sensed by the human host—Beyond conventional antiparasitic therapy. *PLoS One* 7(11):e48418.
30. Clatworthy AE, Pierson E, Hung DT (2007) Targeting virulence: A new paradigm for antimicrobial therapy. *Nat Chem Biol* 3(9):541–548.
31. Carter NS, Yates P, Arendt CS, Boitz JM, Ullman B (2008) Purine and pyrimidine metabolism in *Leishmania*. *Adv Exp Med Biol* 625:141–154.
32. Pfaller MA, Marr JJ (1974) Antileishmanial effect of allopurinol. *Antimicrob Agents Chemother* 5(5):469–472.
33. Carrion R, Jr, Ro YT, Patterson JL (2008) *Leishmaniaviruses. Encyclopedia of Virology*, eds Mahy BWJ, Van Regenmortel MHV (Academic, Amsterdam), pp 220–224.
34. Wickner RB, Ghabrial SA, Nibert ML, Patterson JL, Wang CC (2011) Totiviridae. *Virus Taxonomy: Ninth Report of the International Committee on Taxonomy of Viruses*, eds King AMQ, Lefkowitz E, Adams MJ, Carstens EB (Elsevier, Amsterdam), p 650.
35. Cadd TL, Keenan MC, Patterson JL (1993) Detection of *Leishmania* RNA virus 1 proteins. *J Virol* 67(9):5647–5650.
36. Zangger H, et al. (2013) Detection of *Leishmania* RNA virus in *Leishmania* parasites. *PLoS Negl Trop Dis* 7(1):e2006.
37. Carroll SS, et al. (2003) Inhibition of hepatitis C virus RNA replication by 2′-modified nucleoside analogs. *J Biol Chem* 278(14):11979–11984.

38. Olsen DB, et al. (2004) A 7-deaza-adenosine analog is a potent and selective inhibitor of hepatitis C virus replication with excellent pharmacokinetic properties. *Antimicrob Agents Chemother* 48(10):3944–3953.
39. Eltahla AA, Luciani F, White PA, Lloyd AR, Bull RA (2015) Inhibitors of the hepatitis C virus polymerase; mode of action and resistance. *Viruses* 7(10):5206–5224.
40. Sofia MJ, Chang W, Furman PA, Mosley RT, Ross BS (2012) Nucleoside, nucleotide, and non-nucleoside inhibitors of hepatitis C virus NS5B RNA-dependent RNA-polymerase. *J Med Chem* 55(6):2481–2531.
41. Yin Z, et al. (2009) An adenosine nucleoside inhibitor of dengue virus. *Proc Natl Acad Sci USA* 106(48):20435–20439.
42. Carrion R, Jr, Ro YT, Patterson JL (2003) Purification, identification, and biochemical characterization of a host-encoded cysteine protease that cleaves a *leishmaniavirus* gag-pol polyprotein. *J Virol* 77(19):10448–10455.
43. VanDusen WJ, et al. (1997) Adenine quantitation in yeast extracts and fermentation media and its relationship to protein expression and cell growth in adenine auxotrophs of *Saccharomyces cerevisiae*. *Biotechnol Prog* 13(1):1–7.
44. Fink GR, Styles CA (1972) Curing of a killer factor in *Saccharomyces cerevisiae*. *Proc Natl Acad Sci USA* 69(10):2846–2849.
45. Bhatti MF, et al. (2011) The effects of dsRNA mycoviruses on growth and murine virulence of *Aspergillus fumigatus*. *Fungal Genet Biol* 48(11):1071–1075.
46. Ro YT, Scheffter SM, Patterson JL (1997) Hygromycin B resistance mediates elimination of *Leishmania* virus from persistently infected parasites. *J Virol* 71(12):8991–8998.
47. Wickner RB, Fujimura T, Esteban R (2013) Viruses and prions of *Saccharomyces cerevisiae*. *Adv Virus Res* 86:1–36.
48. Chung IK, et al. (1998) Generation of the short RNA transcript in *Leishmaniavirus* correlates with the growth of its parasite host, *Leishmania*. *Mol Cells* 8(1):54–61.
49. Eldrup AB, et al. (2004) Structure-activity relationship of heterobase-modified 2′-C-methyl ribonucleosides as inhibitors of hepatitis C virus RNA replication. *J Med Chem* 47(21): 5284–5297.
50. Migliaccio G, et al. (2003) Characterization of resistance to non-obligate chain-terminating ribonucleoside analogs that inhibit hepatitis C virus replication in vitro. *J Biol Chem* 278(49):49164–49170.
51. Chen YL, et al. (2010) Inhibition of dengue virus RNA synthesis by an adenosine nucleoside. *Antimicrob Agents Chemother* 54(7):2932–2939.
52. Furman PA, Lam AM, Murakami E (2009) Nucleoside analog inhibitors of hepatitis C viral replication: Recent advances, challenges and trends. *Future Med Chem* 1(8): 1429–1452.
53. Murakami E, et al. (2008) The mechanism of action of beta-D-2′-deoxy-2′-fluoro-2′-C-methylcytidine involves a second metabolic pathway leading to beta-D-2′-deoxy-2′-fluoro-2′-C-methyluridine 5′-triphosphate, a potent inhibitor of the hepatitis C virus RNA-dependent RNA polymerase. *Antimicrob Agents Chemother* 52(2):458–464.
54. Lye L-F, et al. (2010) Retention and loss of RNA interference pathways in trypanosomatid protozoans. *PLoS Pathog* 6(10):e1001161.
55. Ito MM, et al. (2015) Correlation between presence of *Leishmania* RNA virus 1 and clinical characteristics of nasal mucosal leishmaniosis. *Rev Bras Otorrinolaringol (Engl Ed)* 81(5):533–540.
56. Carroll SS, et al. (2009) Robust antiviral efficacy upon administration of a nucleoside analog to hepatitis C virus-infected chimpanzees. *Antimicrob Agents Chemother* 53(3):926–934.
57. Wu B, et al. (2016) *Eimeria tenella*: A novel dsRNA virus in *E. tenella* and its complete genome sequence analysis. *Virus Genes* 52(2):244–252.
58. Nibert ML, Woods KM, Upton SJ, Ghabrial SA (2009) *Cryspovirus*: A new genus of protozoan viruses in the family Partitiviridae. *Arch Virol* 154(12):1959–1965.
59. Ghabrial SA, et al. (2011) Partitiviridae. *Virus Taxonomy: Ninth Report of the International Committee on Taxonomy of Viruses*, eds King AMQ, Adams MJ, Carstens EB, Lefkowitz EJ (Elsevier, Amsterdam), pp 523–534.
60. Livak KJ, Schmittgen TD (2001) Analysis of relative gene expression data using real-time quantitative PCR and the 2(-Delta Delta C(T)) Method. *Methods* 25(4):402–408.
61. Committee on Care and Use of Laboratory Animals (2011) *Guide for the Care and Use of Laboratory Animals* (National Academies Press, Washington, DC), 8th Ed.
62. Appleby TC, et al. (2015) Viral replication. Structural basis for RNA replication by the hepatitis C virus polymerase. *Science* 347(6223):771–775.
63. Meng EC, Pettersen EF, Couch GS, Huang CC, Ferrin TE (2006) Tools for integrated sequence-structure analysis with UCSF Chimera. *BMC Bioinformatics* 7:339.
64. Kelley LA, Mezulis S, Yates CM, Wass MN, Sternberg MJ (2015) The Phyre2 web portal for protein modeling, prediction and analysis. *Nat Protoc* 10(6):845–858.
65. Wass MN, Kelley LA, Sternberg MJ (2010) 3DLigandSite: Predicting ligand-binding sites using similar structures. *Nucleic Acids Res* 38(Web Server issue):W469–473.
66. Lam AM, et al. (2014) Molecular and structural basis for the roles of hepatitis C virus polymerase N55B amino acids 15, 223, and 321 in viral replication and drug resistance. *Antimicrob Agents Chemother* 58(11):6861–6869.
67. Qing J, et al. (2016) Resistance analysis and characterization of NITD008 as an adenosine analog inhibitor against hepatitis C virus. *Antiviral Res* 126:43–54.
68. Dunbrack RL, Jr (2002) Rotamer libraries in the 21st century. *Curr Opin Struct Biol* 12(4):431–440.
69. Leyssen P, De Clercq E, Neyts J (2008) Molecular strategies to inhibit the replication of RNA viruses. *Antiviral Res* 78(1):9–25.
70. Smith DB, et al. (2007) Design, synthesis, and antiviral properties of 4′-substituted ribonucleosides as inhibitors of hepatitis C virus replication: the discovery of R1479. *Bioorg Med Chem Lett* 17(9):2570–2576.
71. Tuttle JV, Tisdale M, Krenitsky TA (1993) Purine 2′-deoxy-2′-fluororibosides as anti-influenza virus agents. *J Med Chem* 36(1):119–125.
72. Smith RA, Sidwell RW, Robins RK (1980) Antiviral mechanisms of action. *Annu Rev Pharmacol Toxicol* 20:259–284.
73. Thio CL (2009) Hepatitis B and human immunodeficiency virus coinfection. *Hepatology* 49(5, Suppl):S138–S145.
74. Razonable RR (2011) Antiviral drugs for viruses other than human immunodeficiency virus. *Mayo Clin Proc* 86(10):1009–1026.
75. De Clercq E, Holý A (2005) Acyclic nucleoside phosphonates: A key class of antiviral drugs. *Nat Rev Drug Discov* 4(11):928–940.
76. De Clercq E (2010) Antiretroviral drugs. *Curr Opin Pharmacol* 10(5):507–515.
77. Walker RT, DeClercq E, Eckstein F (1979) *Nucleoside Analogues Chemistry, Biology, and Medical Applications* (Plenum Press, New York).
78. Kitchin JE, Pomeranz MK, Pak G, Washenik K, Shupack JL (1997) Rediscovering mycophenolic acid: A review of its mechanism, side effects, and potential uses. *J Am Acad Dermatol* 37(3 Pt 1):445–449.
79. Vaughan MH, Steele MW (1971) Differential sensitivity of human normal and malignant cells to 8-azahypoxanthine in vitro. *Exp Cell Res* 69(1):92–96.
80. Nelson JA, Carpenter JW, Rose LM, Adamson DJ (1975) Mechanisms of action of 6-thioguanine, 6-mercaptopurine, and 8-azaguanine. *Cancer Res* 35(10):2872–2878.
81. Shnider BI, et al. (1960) Clinical studies of 6-azauracil. *Cancer Res* 20:28–33.
82. Marr JJ, Berens RL (1983) Pyrazolopyrimidine metabolism in the pathogenic trypanosomatidae. *Mol Biochem Parasitol* 7(4):339–356.
83. Bluemling GR (2011) Part I: Synthesis of Cyclobutyl Nucleoside Analogs That Mimic AZT for Inhibition of the K65R HIV-1 Reverse Transcriptase Mutant. PhD thesis (Emory University, Atlanta, GA).
84. Long PH (1941) The clinical use of sulfanilamide, sulfapyridine, sulfathiazole, sulfaguanidine, and sulfadiazine in the prophylaxis and treatment of infections. *Can Med Assoc J* 44(3):217–227.
85. Durantel D (2009) Celgosivir, an alpha-glucosidase I inhibitor for the potential treatment of HCV infection. *Curr Opin Investig Drugs* 10(8):860–870.
86. Sawyer PR, Brogden RN, Pinder RM, Speight TM, Avery GS (1975) Clotrimazole: A review of its antifungal activity and therapeutic efficacy. *Drugs* 9(6):424–447.

Supporting Information

Kuhlmann et al. 10.1073/pnas.1619114114

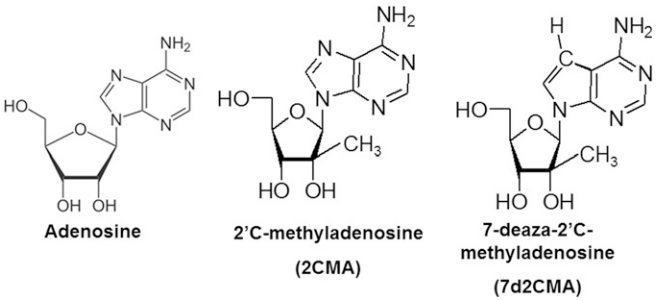

Fig. S1. Structures of compounds showing activity against LRV1 related to adenosine.

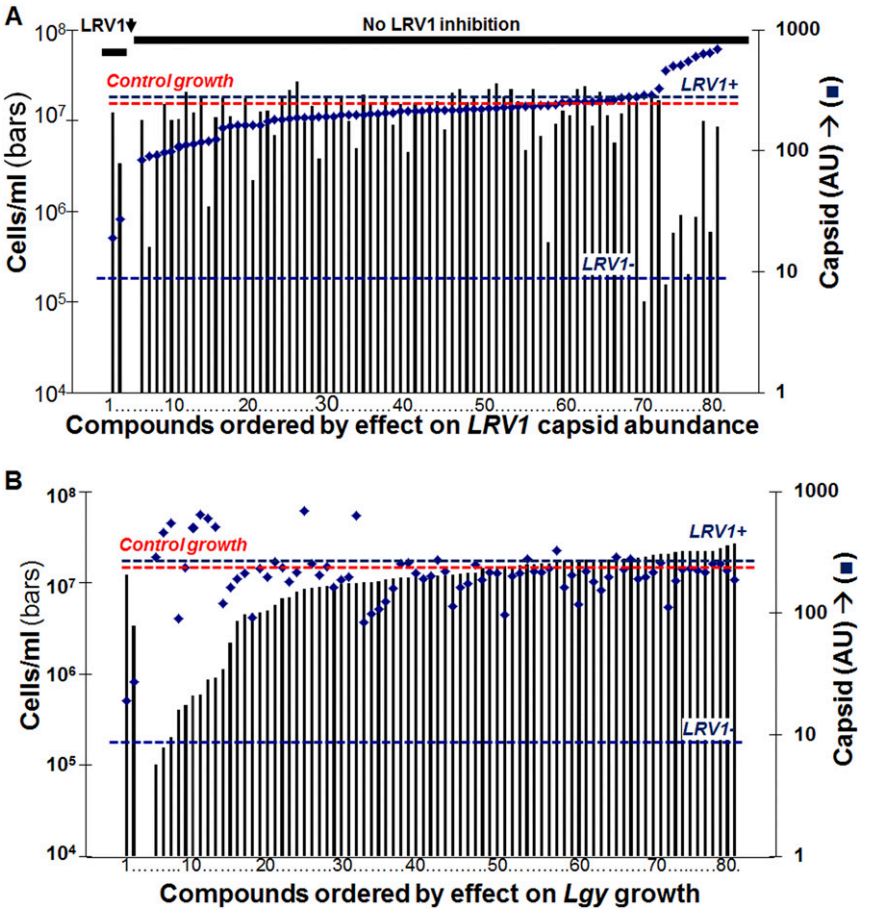

Fig. S2. Inhibition results ordered by effects on relative LRV1 (*A*) or *Leishmania guyanensis* growth (*B*). Dashed lines show the WT control growth rate (red) or *Lgy*LRV1^{+} or *Lgy*LRV1^{-} capsid levels (blue).

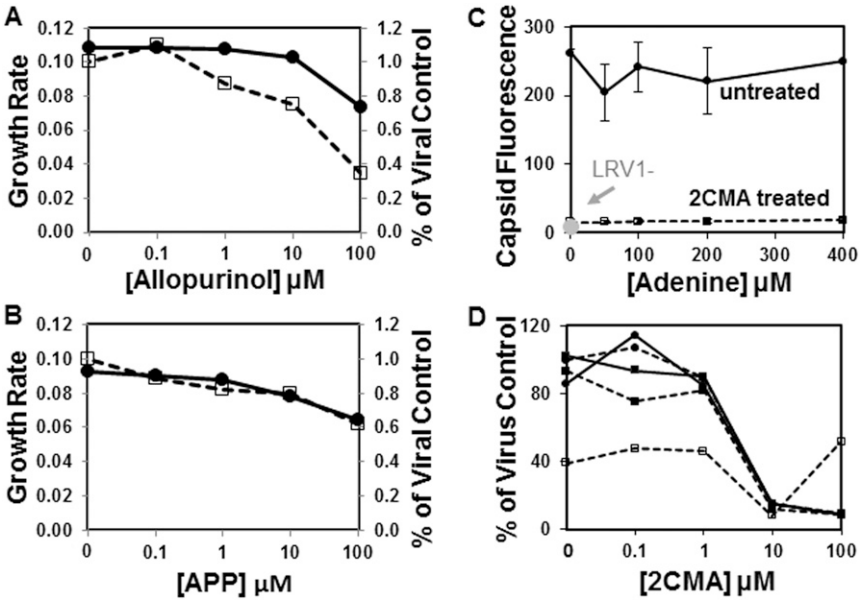

Fig. S3. LRV1 inhibition by 2CMA is insensitive to exogenous adenine and does not show synergy with allopurinol. (*A*) Plot of growth rate of *Lgy*LRV1^{+} (●) or LRV1 capsid levels (○) after 48-h propagation in increasing concentrations of allopurinol. LRV1 percentages were calculated relative to untreated controls. (*B*) As in *A*, but with APP. (*C*) Effect of increasing concentrations of adenine on *Lgy*LRV1^{+} treated with 100 µM 2CMA for six cell doublings (○, dashed line) or without 2CMA (●, solid line). *Lgy*LRV1^{-} (●) is shown for a reference without adenine. (*D*) The EC_{50} for 2CMA inhibition of LRV1 after 48 h is unaltered in the presence of allopurinol. The geometric mean capsid intensity is plotted relative to an untreated control. None (●, solid line), 0.1 µM (■, solid line), 1 µM (●, dashed line), 10 µM (■, dashed line), and 100 µM (○, dashed line). Results from a single experiment are shown, other than *C* ($n = 3$).

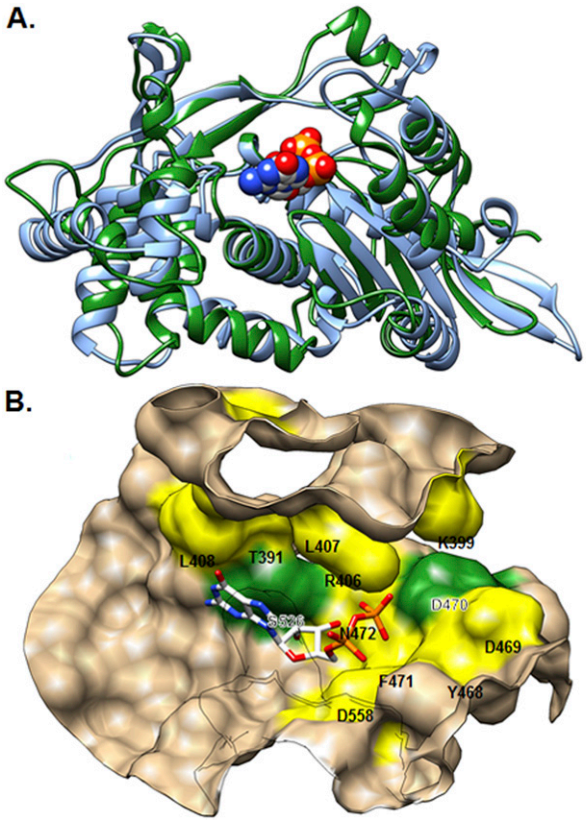

C.

HCV	LRV1
K141	T391
K154	K399
R158	R406
L159	L407
I160	L408
T221	Y468
R222	D469
★C223(H)	**D470**
F224	F471
D225	N472
★S282(T)	**S526**
D318	D558

Fig. S4. Active site model for *L. guyanensis* RDRP. (*A*) Overall structural alignment of the *Lgy* LRV1 RDRP core domain's predicted structure (green) to a crystal structure of the HCV RDRP [light blue; PDB ID code 4WTI (62)] created with the University of California, San Francisco Chimera MatchMaker tool (63). For clarity, only the portion of the HCV RDRP (residues 103–422) that corresponds to the LRV1 RDRP core is shown. The HCV RDRP structure contained bound RNA and GDP. The GDP is shown in this figure to locate the NTP binding pocket. The *L. guyanensis* LRV1 RDRP structure was predicted using the intensive method on the PHYRE2 web service (64), which yielded a high-confidence (≥90%) region between residues 337 and 660. Given just this core region, PHYRE2 produced a very high-confidence structure (100% confidence over 94% of residues) with an active site very similar to the HCV structure. (*B*) Predicted structure of the nucleotide binding pocket in the LRV1 RDRP. The GDP molecule from *A* is shown for clarity. Surface colored yellow represents the locations of residues forming a binding site predicted by the 3DLigandSite server with high confidence (average MAMMOTH score 29.7, where ≥7 is significant) (65). Areas colored green mark residues that, when mutated in the HCV RDRP, confer resistance to the 2′-C-methyl family of nucleoside analogs (50, 66, 67). The "Rotamers" tool in University of California, San Francisco Chimera was used to fix side-chains given unfavorable conformations by the PHYRE2 server (68). (*C*) Table of predicted binding site residues in *Lgy*M4147 LRV1 RDRP and their corresponding residues in the HCV RDRP. Substitutions shown in bold confer resistance to 2′-C-methyl nucleoside analogs in HCV RDRP (50, 66, 67).

Table S1. Compounds studied in this work

Identifier	Alternative names/abbreviations	Pub Chem ID	Uses	Supplier	Source
2′C modified nucleoside/nucleotides					
2′C-Methy adenosine	2CMA, E6	500900	RNAV	G.R.B., Emory University, Atlanta, GA	(51)
2′C-Methyl-7-deaza-adenosine	7d2CMA	3011893	RNAV	Carbosynth	(38)
2′C-Methyl cytidine	2CMC	500902	RNAV	Sigma	(69)
2′C-Methyl guanosine	2CMG, E7	58697480	RNAV	G.R.B., Emory University, Atlanta, GA	(49)
2-((5-(2,4-dioxo-3,4-dihydro-2H-pyrimidin-1-yl)-4-fluoro-3-hydroxy-4–methyltetrahydrofuranyl-2-methoxy) phenoxyphosphorylamino) propionic acid isopropyl ester	PSI-7977, Sofosbuvir	45375808	RNAV	MedChem Express	(39)
2′-Fluoro-2′-methyl-3′,5′-diisobutyryldeoxy cytidine	R-7128, Mericitabine	16122663	RNAV	MedChem Express	(39)
2′-Fluoro-2′-deoxycytidine	E1	101507	RNAV	G.R.B., Emory University, Atlanta, GA	(70)
2′-Fluoro-2′-deoxyinosine	E5	196148	RNAV	G.R.B., Emory University, Atlanta, GA	(71)
2′-Fluoro-2′-deoxyguanosine	E4	196536	RNAV	G.R.B., Emory University, Atlanta, GA	(69)
2′-Fluoro-2′-deoxyadenosine	E3	100253	RNAV, Tumor	G.R.B., Emory University, Atlanta, GA	(71)
2′-Fluoro-2′-deoxyuridine	E2	150851	Tumor	G.R.B., Emory University, Atlanta, GA	(71)
7-(2-Ethynyl-β-D-ribofuranosyl)-7H-pyrrolo[2,3-d]pyrimidine-4-amine	NITD008	44633776	RNAV	BEI Resources	(41)
Other nucleoside/nucleotides					
Ribavirin	Rib	37542	RNAV, DNAV	AKSci	(72)
4′-Azido cytidine	R-1479, Balapiravir	457388	RNAV	MedChem Express	(39)
Entecavir	ETV	153941	DNAV, RTV	LKT Laboratories	(73)
Tenofovir monohydrate	TDF, PMPA	5481350	DNAV, RTV	LKT Laboratories	(73)
Lamivudine	3TC	60825	DNAV, RTV	LKT Laboratories	(73)
Ganciclovir	DHPG,Ganc	3454	DNAV	Sigma	(74)
Cidofovir	CDF	60613	DNAV	Sigma	(75)
Acyclovir	ACY	2022	DNAV	Sigma	(72)
Didanosine	ddi, 2′3′ dideoxyinosine	50599	RTV	LKT Laboratories	(76)
Zidovudine	AZT, azidothymidine	35370	RTV	AKSci	(76)
Stavudine	d4T	18283	RTV	AKSci	(76)
5-Fluoro-5′-deoxyuridine	5F5D, doxifluridine	18343	Tumor	Sigma	(77)
Nucleobase analogs					
Mycophenolic acid	MMA	446541	RNAV, immuno-suppression	Sigma	(78)
8-Azahypoxanthine	8AH	75895	Tumor	Sigma	(79)
5-Azauracil	5AU	6275	Tumor	Sigma	(77)
8-Azaguanine	8AG	8646	Tumor	Sigma	(80)
6-Azauracil	6AU	68037	Tumor	Sigma	(81)
5-Fluorouracil	5FU	3385	Tumor	Sigma	
Allopurinol	ALL	2094	*Leishmania*, gout	Sigma	(82)
4-Aminopyrazolopyrimidine	APP	75420	*Leishmania*	Sigma	(82)
Favipiravir	T-705	492405	RNAV	MedChem Express	(39)
3′-Azido-3′-hydroxyethyl cyclobutyl adenine	E8	No ID		G.R.B., Emory University, Atlanta, GA	(83)

Table S1. Cont.

Identifier	Alternative names/abbreviations	Pub Chem ID	Uses	Supplier	Source
3′-Azido-3′-hydroxyethyl cyclobutyl adenine	E9 (E8 enantiomer)	No ID		G.R.B., Emory University, Atlanta, GA	(83)
3′-Hydroxyethyl cyclobutyl adenine	E10	57450866		G.R.B., Emory University, Atlanta, GA	(83)
Cysteine proteinase inhibitors					
E-64		123985		Cayman Chemical	
E64-d	Aloxistatin	65663		Cayman Chemical	
CA-074 Me		6610318		Enzo Life Science	
Other					
Foscarnet	Phosphono-formic acid	3415	DNAV	LKT Laboratories	(72)
Sulfaguanidine		5324	Antifolate	Sigma	(84)
Celgosivir	6-O-butanoyl castano-spermine	60734	Glucosidase inhibitor	BEI Resources	(85)
Clotrimazole	CTZ	2812	Antifungal	Sigma	(86)
Cycloheximide	CHX	6197	Protein synthesis	A.G. Scientific	
Chembridge (“nucleoside-like library”)					
Chembridge 5106522	CB1	254731		Chembridge	
Chembridge 5135608	CB2	2829334		Chembridge	
Chembridge 5141196	CB31	2998527		Chembridge	
Chembridge 5141213	CB3	249989		Chembridge	
Chembridge 5141214	CB4	330408		Chembridge	
Chembridge 5141245	CB5	2829731		Chembridge	
Chembridge 5141262	CB6	No ID		Chembridge	
Chembridge 5141271	CB7	2829733		Chembridge	
Chembridge 5141274	CB8	2829734		Chembridge	
Chembridge 5141597	CB9	232480		Chembridge	
Chembridge 5141601	CB10	3091582		Chembridge	
Chembridge 5141604	CB11	254686		Chembridge	
Chembridge 5141605	CB12	248866		Chembridge	
Chembridge 5141608	CB13	6612425		Chembridge	
Chembridge 5144558	CB14	259811		Chembridge	
Chembridge 5237407	CB15	5069886		Chembridge	
Chembridge 5312810	CB16	No ID		Chembridge	
Chembridge 5315625	CB17	9585602		Chembridge	
Chembridge 5323146	CB18	2841452		Chembridge	
Chembridge 5482485	CB19	315071		Chembridge	
Chembridge 5487823	CB20	232480		Chembridge	
Chembridge 5489087	CB21	3093658		Chembridge	
Chembridge 5491596	CB22	2849215		Chembridge	
Chembridge 5492915	CB23	2849283		Chembridge	
Chembridge 5493580	CB24	3300105		Chembridge	
Chembridge 5584034	CB25	6095322		Chembridge	
Chembridge 5668881	CB26	2860060		Chembridge	
Chembridge 5670488	CB27	241893		Chembridge	
Chembridge 5671073	CB28	2860348		Chembridge	
Chembridge 5675149	CB29	325243		Chembridge	
Chembridge 5676375	CB30	2861016		Chembridge	
Chembridge 5705708	CB32	325243		Chembridge	

Table S1. Cont.

Identifier	Alternative names/abbreviations	Pub Chem ID	Uses	Supplier	Source
Chembridge 5788245	CB33	286003		Chembridge	
Chembridge 5789784	CB34	283288		Chembridge	
Chembridge 5790592	CB35 N,*N*-dimethyl adenosine	348206		Chembridge	
Chembridge 5790637	CB36	2868728		Chembridge	
Chembridge 5790716	CB37	286481		Chembridge	
Chembridge 7972230	CB38	2978428		Chembridge	
Chembridge 7978592	CB39	2980412		Chembridge	

DNAV, DNA viruses; RNAV, RNA viruses; RTV, retroviruses.

Table S2. Parasite growth and LRV1 levels in response to test compounds

Compound	Abbr.	Stock (mM)	Solvent	Tested (μM)	Density (cells/mL)	Percent control	LRV1 capsid (geometric mean FU)	Percent control	LRV1 rank (Fig. S2*A*)	Growth rank (Fig. S2*B*)
2′C-methyadenosine	E6/2CMA	50	DMSO	100	1.22E+7	72	19	7	1	1*
2′C-methyl-7-deaza-adenosine	7d2CMA	100	DMSO	100	3.38E+6	20	27	10	2	2*
CA-074-Me	CP3	25	DMSO	50	1.00E+07	60	83	31	3	31
Allopurinol	ALL	50	DMSO	100	4.06E+5	2	90	34	4	6
Chembridge 5670488	CB27	50	DMSO	100	4.59E+6	27	91	34	5	16
e64d	CP2	5	DMSO	10	1.52E+07	90	97	37	6	50
NITD008	NITD008	50	DMSO	1	1.02E+7	61	98	37	7	32
Chembridge 5141196	CB31	50	DMSO	100	1.05E+7	62	108	41	8	33
Chembridge 5315625	CB17	50	DMSO	100	2.08E+7	123	113	42	9	72
R-1479	R-1479	50	DMSO	100	1.23E+7	73	114	43	10	43
Entecavir	ETV	50	DMSO	100	1.77E+7	105	119	45	11	60
APP	APP	50	DMSO	50	1.12E+6	7	119	45	12	12
Celgosivir	Celgosivir	50	DMSO	10	1.09E+7	65	124	47	13	34
e64	CP1	25	DMSO	50	1.80E+07	107	153	58	14	63
T-705	T-705	50	DMSO	100	1.13E+7	67	161	60	15	35
Foscarnet	Fosc	50	DMSO	100	9.50E+6	56	162	61	16	27
2′C-Methylcytidine	2CMC	100	DMSO	100	1.73E+7	103	162	61	17	58
Ribavirin	Rib	50	Water	100	2.21E+6	13	162	61	18	13
PSI-7977	PSI-7977	50	DMSO	100	1.25E+7	74	163	61	19	44
R-7128	R-7128	50	DMSO	100	1.27E+7	76	175	66	20	45
Chembridge 5676375	CB30	50	DMSO	100	6.93E+6	41	181	68	21	21
Didanosine	ddi	50	DMSO	100	1.80E+7	107	182	68	22	62
Chembridge 5482485	CB19	50	DMSO	100	2.18E+7	129	183	69	23	73
Chembridge 5323146	CB18	50	DMSO	100	2.66E+7	158	186	70	24	81
Chembridge 5675149	CB29	50	DMSO	100	9.57E+6	57	187	71	25	28
Chembridge 5671073	CB28	10	DMSO	20	1.46E+7	87	189	71	26	47
Chembridge 7978592	CB39	50	DMSO	100	3.77E+6	22	189	71	27	14
Chembridge 5141214	CB4	50	DMSO	100	1.88E+7	112	190	72	28	68
Chembridge 5788245	CB33	25	DMSO	50	1.17E+7	69	192	72	29	39
Zidovudine	AZT	50	Water	100	1.81E+7	107	196	74	30	64
Ganciclovir	Ganc	20	DMSO	40	9.78E+6	58	198	75	31	229
Chembridge 5106522	CB1	50	DMSO	100	4.98E+6	30	199	75	32	18
Chembridge 5141608	CB13	50	DMSO	100	1.92E+7	114	199	75	33	69
Chembridge 5492915	CB23	10	DMSO	100	1.52E+7	90	202	76	34	51
Chembridge 5790637	CB36	50	DMSO	100	1.19E+7	71	203	77	35	40
Chembridge 5141597	CB9	50	DMSO	100	1.75E+7	104	206	77	36	59
Tenofovir	TDF	50	DMSO	100	8.90E+6	53	206	78	37	25
Chembridge 5584034	CB25	50	DMSO	100	1.50E+7	89	212	80	38	49
Chembridge 5312810	CB16	10	DMSO	20	4.46E+6	27	212	80	39	15
Chembridge 5489087	CB21	50	DMSO	100	1.57E+7	93	213	80	40	52
Chembridge 5789784	CB34	25	DMSO	50	1.16E+7	69	214	81	41	38
Chembridge 5668881	CB26	25	DMSO	50	1.49E+7	89	215	81	42	48
Chembridge 5141262	CB6	50	DMSO	100	1.61E+7	96	215	81	43	55
Chembridge 5790716	CB37	50	DMSO	100	7.91E+6	47	216	81	44	22
Chembridge 5487823	CB20	50	DMSO	100	2.03E+7	121	216	81	45	70
Chembridge 5144558	CB14	50	DMSO	100	2.24E+7	133	217	82	46	77
Stavudine	d4T	50	EtOH	100	1.60E+7	95	220	83	47	54
Chembridge 5141213	CB3	50	DMSO	100	1.80E+7	107	220	83	48	61
Chembridge 5493580	CB24	50	DMSO	20	1.21E+7	72	222	84	49	42
Chembridge 5141604	CB11	50	DMSO	100	2.24E+7	133	223	84	50	76
Chembridge 5141605	CB12	50	DMSO	100	2.56E+7	152	225	85	51	80
Chembridge 5237407	CB15	50	DMSO	100	1.82E+7	108	227	86	52	66
2′-Fluoro-2′-deoxycytidine	E1	50	DMSO	100	2.21E+7	132	230	87	53	74
Chembridge 5491596	CB22	50	DMSO	100	1.62E+7	97	232	87	54	56
5-Fluoro-5′-deoxyuridine	5F5D	50	DMSO	100	4.71E+6	28	234	88	55	17
2′-fluoro-2′-deoxyuridine	E2	50	DMSO	100	2.22E+7	132	234	88	56	75
Chembridge 7972230	CB38	50	DMSO	100	6.67E+6	40	236	89	57	20
Mycophenolic acid	MMA	50	DMSO	1	4.55E+5	3	238	90	58	7

Table S2. Cont.

Compound	Abbr.	Stock (mM)	Solvent	Tested (μM)	Density (cells/mL)	Percent control	LRV1 capsid (geometric mean FU)	Percent control	LRV1 rank (Fig. S2*A*)	Growth rank (Fig. S2*B*)
Lamivudine	3TC	50	DMSO	100	9.20E+6	55	242	91	59	26
8-Azahypoxanthine	8AH	50	DMSO	100	1.29E+7	77	251	95	60	46
5-Azauracil	5AU	50	DMSO	100	1.13E+7	67	252	95	61	36
2′C-Methyguanosine	E7	50	DMSO	100	2.25E+7	133	252	95	62	78
2′-Fluoro-2′-deoxyinosine	E5	50	DMSO	100	2.41E+7	143	255	96	63	79
Chembridge 5705708	CB32	50	DMSO	100	8.69E+6	52	255	96	64	24
2′-Fluoro-2′-deoxyadenosine	E3	50	DMSO	100	2.07E+7	123	257	97	65	71
Sulfaguanidine	None	50	DMSO	100	1.15E+7	68	260	98	66	37
8-Azaguanine	8AG	50	DMSO	100	5.68E+6	34	264	100	67	19
6-Azauracil	6AU	50	DMSO	100	1.20E+7	71	271	102	68	41
3′-Azido-3′-hydroxyethyl cyclobutyl adenine	E8	50	DMSO	100	1.86E+7	111	277	104	69	67
3′-Azido-3′-hydroxyethyl cyclobutyl adenine	E9	50	DMSO	100	1.58E+7	94	279	105	70	53
Chembridge 5790592	CB35	50	DMSO	100	1.00E+5	1	287	108	71	3
3′-Hydroxyethyl cyclobutyl adenine	E10	50	DMSO	100	1.82E+7	108	290	109	72	65
2′-fluoro-2′-deoxyguanosine	E4	50	DMSO	100	1.68E+7	100	326	123	73	57
Chembridge 5135608	CB2	50	DMSO	100	1.55E+5	1	460	173	74	4
Chembridge 5141601	CB10	50	DMSO	100	5.72E+5	3	502	189	75	8
5-Fluorouracil	5FU	50	DMSO	100	9.05E+5	5	512	193	76	11
Chembridge 5141274	CB8	50	DMSO	100	2.02E+5	1	547	206	77	5
Chembridge 5141245	CB5	50	DMSO	100	8.73E+5	5	603	227	78	10
Cidofovir	CDF	10	40% DMSO, 0.1 mM NaOH	40	9.99E+6	59	637	240	79	30
Chembridge 5141271	CB7	50	DMSO	100	5.85E+5	3	650	245	80	9
Acyclovir	ACY	30	DMSO	120	8.55E+6	51	687	259	81	23
*Lgy*LRV1^{+} CONTROL	LRV1^{+}	N/A	N/A	N/A	1.68E+07	100	265	100	N/A	N/A
*Lgy*LRV1^{-} CONTROL	LRV1^{-}	N/A	N/A	N/A	1.42E+07	85	9	3	N/A	N/A

Compound names and abbreviations (Table S1) are provided in column 1. Inhibitors were dissolved and used as indicated in column 2. Parasite density was measured after 2 d in culture and normalized to the percent growth of the diluent-treated control in column 3. LRV1 capsid signal was assessed at the same time as growth in column 4. Columns 5 and 6 provide the rank position for each compound as depicted in Fig. S2. Red shading represents inhibition of *L. guyanensis*. Green shading represents inhibition of LRV1. Yellow shading denotes control parameters. N/A, not applicable.
*Actual rank: 1 = 42, 2 = 12.